Dynamics of water storage in mature subalpine *Picea abies*: temporal and spatial patterns of change in stem radius

R. ZWEIFEL[1] and R. HÄSLER[2,3]

[1] *Institute of Plant Sciences, University of Bern, Altenbergrain 21, CH-3013 Bern, Switzerland*

[2] *Swiss Federal Research Institute WSL, Zürcherstrasse 111, CH-8903 Birmensdorf, Switzerland*

[3] *Author to whom correspondence should be addressed*

Summary Internal water reserves in bark and foliage of trees contribute to transpiration (T) and play an essential role in optimizing water transport by buffering extreme peaks of water consumption. We examined patterns of stem shrinkage and their relationship to tree water dynamics. We measured fluctuations in root radius and stem radius at different stem heights, T of twigs at the top of the crown and sap flow velocities in stem sections of mature subalpine Norway spruce (*Picea abies* (L.) Karst.) trees over 2 years. The output of each sensor was coupled by physical functions to a mechanistic flow and storage model of tree water relations. The data verified the model-predicted lag in water storage depletion in response to the onset of transpiration and the lag increased with increasing distance from the crown periphery. Between the crown and stem base, the delay ranged from a few minutes to several hours, depending on microclimatic conditions and tree water status. Stem volume changes were proportional to the amount of water exchanged between the elastic tissues of the bark and the rigid xylem, indicating that the "peristaltic" wave of stem contraction along the flow path represented depletion of water stored in bark. On a daily basis, stems lost between 0.2 and 0.5% of their volume as a result of bark dehydration, corresponding to about 2 to 5 l of water. This water contributed directly to T. According to the model based on hydraulic principles, there are three main components underlying the dynamics of water storage depletion: flow resistance, storage capacities of needles and bark, and T of each tree section. The resistances and capacities were proportional to the response delay, whereas T in the lower parts of the tree was inversely proportional. The pattern of T within the crown depended on water intercepted by the branches. Because of these weather-dependent factors, there was no time constant for the response delay along the flow path. Nevertheless, the upper crown and the root section tended to have longer response delays per meter of flow path than the stem. The diurnal course of stem radius fluctuations represents the sum of all external and internal conditions affecting tree water relations; stem radius fluctuations, therefore, provide a sensitive measure of tree water status.

Keywords: bark dehydration, conifers, dendrometer, tissue contraction, water relations.

Introduction

Water relations of trees are determined, in part, by the availability of internal water reserves for transpiration. Every day, needles (Nakayama and Ehrler 1963, Hinckley et al. 1978, Boyce et al. 1991, Gross and Koch 1991) and bark (Herzog et al. 1995, Köstner et al. 1998, Zweifel 1999) swell overnight and shrink during the transpiration period, because water from internal storage locations plays a direct role in the daily turnover of water in a tree. Investigating the interactions between these internal storage locations and other components of the water balance is an important step in understanding tree reactions to changing environmental conditions.

Although variations in needle water content in a tree crown are difficult to record automatically, diurnal dynamics of bark water contents can be measured as fluctuations in stem radius. In Norway spruce (*Picea abies* (L.) Karst.), the amplitude of diurnal fluctuations in stem radius varies between 20 and 200 μm (Herzog et al. 1997, Zweifel 1999) over the growing season and by up to more than 1 mm in winter (Zweifel and Häsler 2000). Several authors have reported that stem radius changes occur mainly in the elastic tissue of the bark (Dobbs and Scott 1971, Molz and Klepper 1973, Zweifel et al. 2000), whereas the woody parts of the stem undergo only small diurnal fluctuations (Siau 1984, Irvine and Grace 1997). These findings suggest that the resulting stem volume changes also take place mainly in the bark. Zweifel et al. (2000) found that, in young *P. abies*, bark volume is proportional to bark water content provided that the xylem water potential (Ψ_S) is more than -2.3 ± 0.3 MPa. Thus, it is possible to estimate rates of water depletion and replenishment of water in the bark from continuous dendrometer measurements of stems.

The flow and storage of water in trees can be modeled as an electrical circuit (Larcher 1995, Williams et al. 1996, Loustau et al. 1998) or as a hydraulic system (Jarvis 1975, Edwards et al. 1986, Tyree 1988, Früh 1995, Zweifel 1999). Both models connect the different system components by physical, chemical or physiological causalities only. The present work is based on a hydraulic model that consists of storage locations and flow path sections. In this model, water storage pools are defined by their storage capacity and ability to retain water

against a water potential gradient. These gradients within the flow path or between storage compartments force water to move according to Darcy's law. At absolute water potentials near zero, the storage locations are saturated and water is no longer forced to move within the plant. Zweifel (1999) successfully simulated the diurnal course of stem radius changes of young conifers based on the course of transpiration with such a functional model. The model comprised only one bark storage location, one crown storage location, and the flow path between them. The soil water potential and the water demand of the air determined the boundary conditions.

A mechanistic model of similar design and simplicity was used in the present study. The model has been improved by using several segments, each comprising a flow path section, a bark storage location and a crown storage (needles) location. Water is transported into the next upper (stem) segment and it is partially transpired through the needles of the branches. Segments of the lower tree parts might be excluded from crown storage and also water loss by transpiration because of their lack of branches. In the model, water hydraulically connects every plant part and any disturbance to the water balance affects the whole system (Jarvis 1975). For example, transpiration in the crown top starts a chain of events involving water storage depletion and water flow throughout the tree. Response delays following the onset of transpiration should theoretically be detectable along tree stems and roots, depending on flow resistances and storage capacities. Model results of storage dynamics in trees (Edwards et al. 1986, Tyree 1988) and investigations with potted *P. abies* (Zweifel 1999) indicate the existence of such a "peristaltic" wave of storage depletion at ever increasing distances from the crown periphery. However, little is known about the dynamics of stem radius fluctuations along the stem and roots of mature trees.

In the present investigation, we continuously recorded the dynamics of stem radius fluctuations in mature, subalpine *P. abies* trees over 2 years. We modeled the temporal and spatial patterns of water storage dynamics by means of a flow and storage model and show how continuous stem radius measurements can be used to interpret the functionality of tree water relations. Finally, we quantified the daily, seasonal and annual amounts of bark water depletion in relation to bark thickness and annual wood growth.

Materials and methods

Study site and trees

The study site is located at the foot of Mt. Seehorn in a subalpine Norway spruce forest, 1640 m a.s.l. near Davos, Switzerland (46°48′59″ N, 9°51′25″ E). The eight mature (150 to 250 years old) Norway spruce (*Picea abies* (L.) Karst.) trees studied are growing on a slight slope facing toward Mt. Seehorn, which lies to the east of the site. The soil is classified as a ferric humic podsol (Häsler et al. 1991). The organic layer is between 0.1 and 0.4 m deep. Details of stem size and tree height are listed in Table 1.

Table 1. Tree height (h), stem diameter at 1.5 m above ground ($\varnothing_{\text{Stem}1.5m}$), and estimated stem volume (ΔV_{stem}) for the eight study trees of *P. abies*.

Tree	h (m)	$\varnothing_{\text{Stem 1.5m}}$ (m)	ΔV_{Stem} (m^3)
A	25	0.398	1.15
B	23	0.294	0.57
C	24	0.369	0.95
D	25	0.493	1.73
F	15	0.207	0.17
G	13	0.162	0.10
X	28	0.500	2.03
Y	24	0.484	1.59

Measurement concept

The arrangement of measurement instruments within the study site follows the principles of the systemic approach: a few trees were equipped with a combination of many different measurement sensors to investigate tree water relations. The output of every sensor was linked to the model by physical, chemical or physiological functions. To analyze the continuously recorded data, we used diurnal courses whenever possible. We did not average the values to minimize loss of information. The dynamics of the curves were qualitatively tested in the model to determine whether the functional connections between the water balance components can explain all the various phenomena observed. In addition to the trees with many sensors, five trees were equipped with one dendrometer at breast height. The data gathered enabled us to estimate the amount of variation among trees and made it possible to minimize the risk of unknowingly investigating an abnormal tree.

Point dendrometer

From July 1997 to June 1999, twenty point dendrometers (Agricultural Electronics Corp., Tucson, AZ) were used to measure stem and root radius fluctuations (ΔR) continuously. Each stem of the eight trees investigated was equipped on its west side with a point dendrometer at breast height and additional dendrometers were mounted at 6, 10, 14 and 18 m above ground and on roots of trees A, C and F. The dendrometers operated on the basis of a linear variable differential transformer enclosed in an enamel housing on three sides (Gensler and Diaz-Munoz 1983). Three stainless steel threaded rods were implanted to a depth of about 70 mm into the xylem and connected by mounting struts to the tree. The sensing rod was lightly pressed against the stem of the tree by a force unit. The bias caused by hygroscopic swelling and shrinkage of the bark at its surface was minimized by placing the contact point 2 to 6 mm below the surface, but still within the dead outermost layer of the bark. To minimize temperature sensitivity of the dendrometers, we corrected the stem radius measurements with control measurements derived from dendrometers of the same type mounted on a stone plate and a thin steel plate (3 mm), which for the purposes of this study we considered

non-contracting and non-expanding. The bias was linearly correlated to air temperature; an increase of 1 °C caused a mean contraction (artifact) of 1.4 μm. The resolution of the dendrometers was 3.7 μm. The dendrometer data were generally collected at 15-min intervals. On 7 days in the summers of 1997 and 1998, the recording interval was reduced to 2 min.

To obtain additional and independent measurements of stem radius changes, we used three point dendrometers consisting of a precision displacement transducer (TRANS-TEK, Ellington, CT) and a body of stainless steel. The instruments were mounted in the same way as the other dendrometers but the sensing head was glued with tar to the smoothed bark surface of trees A, F and G. The resolution of these dendrometers was 1.5 μm and the recording frequency was 10 min.

Sap flow measurements

In July 1999, three sap flow velocity sensors were mounted at 1.5, 6 and 14 m on the south side of the stem of tree A. The thermal dissipation probe heated needle is an improved heat dissipation sensor, as proposed by (Granier 1985). The probe measures sapwood heat dissipation, which increases with sap flow and the resulting cooling of the heat source, as the apparent thermal conductance of sapwood increases with sap velocity. The data were recorded at 5-min intervals.

Gas exchange chamber

Transpiration rates (T) of two upper-canopy twigs on the south side of the crown of tree A (23 m above ground) were continuously measured over 2 years by means of air-conditioned gas exchange chambers (System Koch, Walz, Germany) (Häsler et al. 1991). Each twig had a leaf area of about 0.2 m² . Data were collected at 5-min intervals.

Extraction of bark and wood cores

Cores of bark and wood (four to eight growth rings) were extracted with an increment corer (Forster et al. 2000) at a distance of approximately 0.05 m from each dendrometer. The cores, which were 8 to 10 mm in length and 1.5 mm in diameter, were used to measure the thickness of bark and growth rings for 1997 and 1998.

Calculation of stem volumes

To calculate stem volumes, we approximated the stem shape by a function for the radius $r(h) = ah^2 + bh + c$, with tree height (h) as the independent variable. The function $r(h)$ was fitted to the stem radius measurements of trees A, B, C and F ($R^2 > 0.98$ for all four trees). Parameters a, b and c for the other trees were obtained by interpolation, based on h and ΔR at 1.5 m above ground as reference values. Stem volume V_{stem} was then calculated as an integral of $r(h)$ over tree height. To estimate stem volume changes (ΔV_{stem}), we multiplied the values of $\Delta R_{1.5m}$ by a factor of 1.3. The factor was estimated from measurements made on trees A and C and took into account that the stem radius fluctuations at 1.5-m height were less than the mean amplitudes of ΔR in higher stem sections.

Results

Temporal and spatial patterns of radius fluctuations along stems and roots

Fluctuations in stem and root radius, as measured with point dendrometers, showed both spatial and temporal patterns. Figure 1a illustrates a spatial pattern for 14 days in August 1997, based on data from seven radius measurement locations along the stem and one root of tree A. Every time interval of a couple of days had its own typical rhythm of stem shrinkage and expansion in which the dynamics of the stem radius fluctuations at different heights were similar but not identical. There were some important quantitative and qualitative differences between the curves: the amplitudes varied with height (Figure 1b) and the diurnal fluctuations followed slightly individual courses. The greatest amplitudes in the diurnal fluctuations in radius occurred in the upper stem part, within the crown, and the lowest amplitudes were detected at the stem base. Roots had similar diurnal fluctuations in radius to the stems.

In addition to the spatial pattern of fluctuations in stem and radius, there was also a temporal pattern. The onset of stem shrinkage (marked with arrows in Figure 2) showed a signifi-
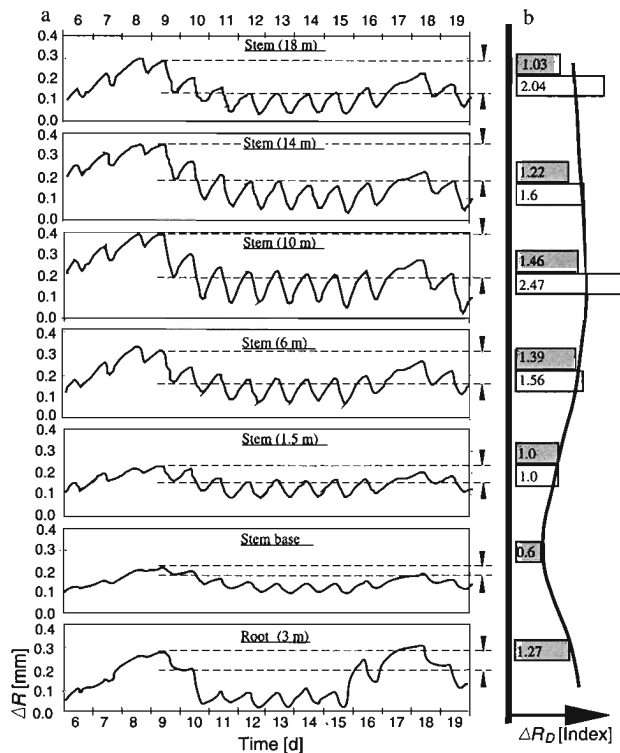

Figure 1. (a) Patterns of radius fluctuations (ΔR) recorded over 14 days at different stem heights and on one root of tree A. The measuring point on the root was located 3 m from the trunk. The amplitudes of the diurnal fluctuation from August 9, 1997 are marked by broken lines and depicted in (b) as bars (ΔR_D). The shaded bars represent tree A and the open bars represent tree C. The black line indicates the mean tendency of the amplitudes with stem height. Values of ΔR_D are normalized so that the records at 1.5 m above ground are equal to 1.0.

cant delay in response to the onset of transpiration from the treetop downward. There was a "peristaltic" wave of contraction along the stem and roots at ever increasing distances from the crown periphery. A similar phenomenon was also detected with sap flow sensors along the stem (data not shown). However, the response delay along the tree cannot be described as a constant value per meter of flow path (Figure 3). Values were much higher at the treetop and also in the rooting zone than in the middle section of the stem. The dynamics of the "peristaltic" wave differed among similar trees and even between trees growing close together. Trees A and C grew within 5 m of each other. On July 21, 1998, for instance (Figure 2), the onset of stem shrinkage at a height of 18 m occurred at 0800 h in tree A and 14 min earlier in tree C. The response delay between 18 m and 1.5 m was 48 min for tree A and only 28 min for tree C. In general, the onset of shrinkage occurred in the same spatial sequence from the treetop downward, whereas the onset of replenishment did not show a regular pattern. The onset of expansion was sometimes observed in the crown and sometimes in the lower stem parts or even in the roots.

Annual dynamics of radius fluctuations

An additional overlaid pattern of stem radius changes was observed when the perspective was increased from diurnal dynamics to a period of more than a year (Figure 4). The annual pattern was mainly determined by the combination of water-
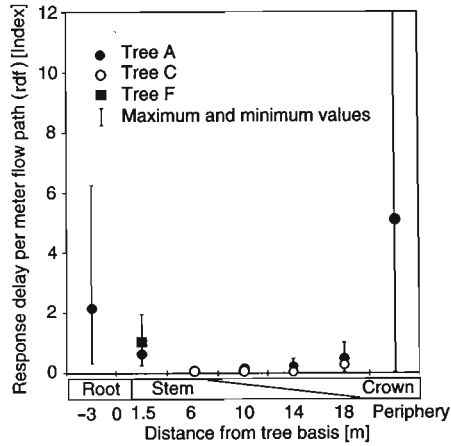

Figure 3. Variation in the response delay factor per meter of flow path (rdf) along the flow path (x axis). There was a tendency toward a higher rdf in the upper crown and roots than in the stem. The response delay factor is dimensionless and is calculated as the measured time delay divided by the number of meters between the two measurement points.

and growth-induced changes in stem radius, and it also included the much greater radius fluctuations in winter compared with summer. Maximum stem shrinkage during a growing season (ΔR_V) lasted from several days (summer 1998) to several weeks (summer 1997) and exceeded the diurnal fluctuations (ΔR_D) by two to four times (Table 2). Maximum stem shrinkage over a year (ΔR_Y) was mainly determined by the large stem contractions in winter (1 to 2 mm). Thus, water-induced shrinkage of the bark reached values up to twice the annual growth-induced increase in stem radius. The ΔR-values listed in Table 2 represent differences between a radius maximum and a following minimum. In this way, it was possible to avoid confusing radius changes caused by water loss or replacement with those caused by wood growth. A negative consequence of adopting this basis for expressing ΔR is that all values are underestimated because of the diametrical direction of wood growth and bark shrinkage.

The thickness of the elastic part of the bark varied widely among trees and also among different measurement points on the same stem. Although there was no significant correlation between bark thickness and the amplitudes of diurnal fluctuations in stem radius, bark thickness tended to be proportional to the amplitudes of the diurnal stem radius variations. Both stem radius fluctuations and bark thickness were maximal in the middle sections of the stems between 6 and 14 m (Table 2 and Figure 1).

Quantification of water storage in stem bark

Absolute amounts of water depleted from bark storage were estimated on the basis of a proportional relationship between stem (bark) dimension and stem (bark) dehydration. Table 3 lists the maximum amounts of water depleted from bark storage over a single day (ΔW_D), over a growing season (ΔW_V), and over a year (ΔW_Y). The amount of water depleted from
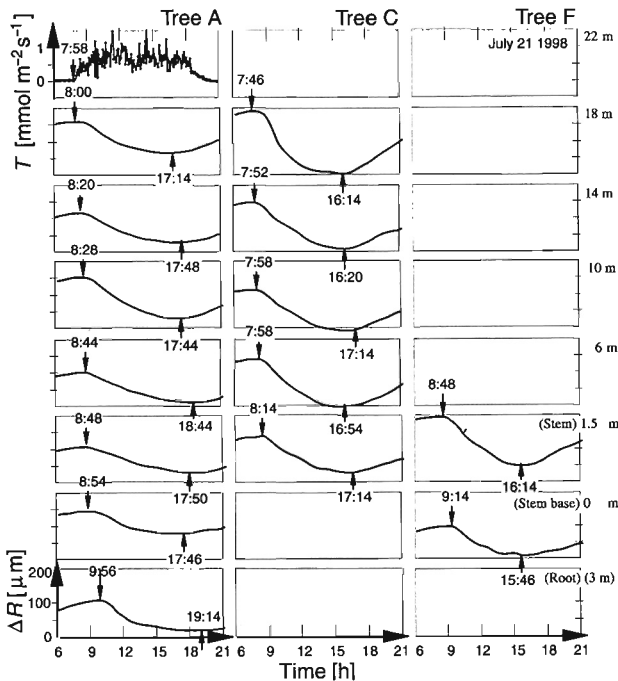

Figure 2. Courses of radius fluctuations (ΔR) along the flow paths of trees A, C and F on a partially sunny day in July 1998. Transpiration rate was measured on a single twig in the crown top. Arrows pointing downward mark the onset of stem shrinkage in the morning at each stem height. Arrows pointing upward mark the onset of stem expansion in the evening.
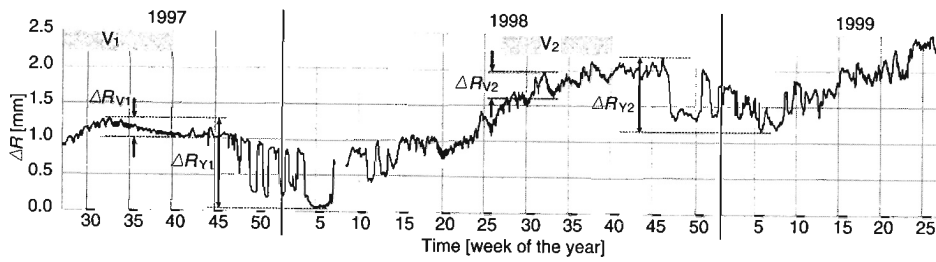
Figure 4. Two-year course of stem radius fluctuations measured with a point dendrometer at 1.5 m above ground on Tree A. Subscripts V_1, V_2 and Y_1, Y_2 mark the main growing periods (July 1 to October 1) and were used to determine ΔR_V, the maximum stem shrinkage over a growing season and ΔR_Y, the maximum stem shrinkage over a year (July 1 to May 31), respectively.

bark storage during the growing season (ΔW_V) amounted to only about 10% of the water depleted over a year (ΔW_Y). Although water depletion periods during the summer (ΔW_V) lasted from several days to a few weeks, the amount of water lost within this time was at most only twice the amount depleted over a single day (ΔW_D). Mean growth ring width (1997 and 1998) of the *P. abies* trees investigated was 0.75 mm, whereas the maximum shrinkage of the bark reached up to 2 mm per year (Table 2). Consequently, the water-induced

shrinkage (or swelling) of the bark exceeded the growth-induced expansion of the wood more than twofold. The diurnal rhythm of storage depletion and replenishment can easily be ascribed to the water-induced stem fluctuations, whereas the periods of stem swelling, extending over several days, are not easy to distinguish from growth. In spring, when the dehydrated bark is replenished and wood growth is simultaneously initiated, it was impossible to differentiate water-induced radius expansion from growth-induced radius expansion in

Table 2. Maximum measured radius contractions of stems and roots over a single day (ΔR_D), over 3 months of the vegetative growth period (ΔR_V) and over 1 year (ΔR_Y). The widths of the corresponding tree rings are listed for the years 1997 and 1998. The bark thickness includes only the elastic tissues phloem and parenchyma but not the dead inelastic outermost layer (periderm) of the bark. Measurement periods: I = July 1, 1997–September 30, 1997; II = July 1, 1997–May 31, 1998; III = July 1, 1998–May 31, 1999; and IV = July 1, 1998–September 30, 1998. Abbreviation: nm = not measured.

Tree		$\Delta R_{D1}{}^{I}$ (μm)	$\Delta R_{D2}{}^{IV}$ (μm)	$\Delta R_{V1}{}^{I}$ (μm)	$\Delta R_{V2}{}^{IV}$ (μm)	$\Delta R_{Y1}{}^{II}$ (μm)	$\Delta R_{Y2}{}^{III}$ (μm)	Tree ring 97 (μm)	Tree ring 98 (μm)	Bark (mm)
$A_{18\,m}$		131	133	525	195	1571	1312	530	730	5.7
$A_{14\,m}$		166	147	485	211	1455	1463	700	770	6.2
$A_{10\,m}$		195	180	593	323	1603	1628	710	610	6.6
$A_{6\,m}$		161	195	371	525	1391	1620	440	520	6.4
$A_{1.5\,m}$		95	162	241	256	1250	1049	520	780	4.7
$A_{0\,m}$	(Root)	75	79	158	179	532	655	450	560	4.6
$A_{-3\,m}$	(Root)	190	137	303	340	438	664	350	550	2.5
$B_{1.5\,m}$		129	135	nm	nm	nm	nm	580	490	2.8
$C_{18\,m}$		nm	279	nm	666	nm	1983	1250	860	5.9
$C_{14\,m}$		nm	219	nm	361	nm	1560	750	1060	6.0
$C_{10\,m}$		nm	338	nm	535	nm	1558	770	810	4.5
$C_{6\,m}$		nm	214	nm	503	nm	1244	650	560	5.6
$C_{1.5\,m\,(NE)}$		142	nm	207	nm	984	nm	940	880	4.6
$C_{1.5\,m\,(NW)}$		122	137	374	294	1228	1218	740	680	5.4
$C_{1.5\,m\,(S)}$		89	nm	176	nm	870	nm	980	1200	4.1
$D_{1.5\,m}$		190	nm	nm	nm	nm	nm	1000	1140	5.9
$F_{1.5\,m\,(NE)}$		92	195	nm	333	1135	1300	710	820	2.3
$F_{1.5\,m\,(W)}$		nm	90	nm	161	nm	723	1050	810	3.3
$F_{1.5\,m\,(SE)}$		nm	nm	nm	498	nm	1151	900	630	3.8
$F_{-0.5\,m\,(SW)}$	(Root)	107	111	210	nm	575	nm	nm	nm	nm
$F_{-0.5\,m\,(NE)}$	(Root)	115	126	147	283	550	530	nm	nm	nm
$F_{-0.5\,m\,(S)}$	(Root)	nm	nm	nm	261	nm	nm	nm	nm	nm
$G_{1.5\,m}$		nm	112	nm	nm	759	1015	700	500	2.6
$X_{1.5\,m}$		130	134	nm	195	1214	nm	850	870	5.8
$Y_{1.5\,m}$		131	163	nm	384	1030	1145	820	790	6.7

Table 3. Maximum, measured, water depletion rates of the stem bark over a single day (ΔW_D), over 3 months of the growing season (ΔW_V), and over 1 year (ΔW_Y) and the corresponding percentage changes in stem volume. Abbreviation: nm = not measured.

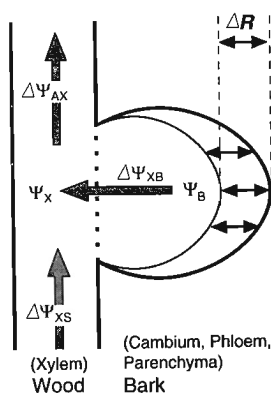| Tree	ΔW_D		ΔW_V		ΔW_Y	
	(l)	(%)	(l)	(%)	(l)	(%)
A	2.8	0.2	5.4	0.5	25.1	2.2
B	1.9	0.3	3.6	0.6	16.9	3.0
C	2.5	0.3	6.5	0.7	23.8	2.5
D	5.1	0.3	nm	nm	nm	nm
F	0.9	0.5	2.1	1.2	7.9	4.6
G	0.5	0.5	nm	nm	4.1	4.1
X	4.0	0.2	6.0	0.3	37.3	1.8
Y	3.7	0.2	9.6	0.6	27.3	1.7

Figure 5. Balloon model, based on hydraulic principles, of the depletion and replenishment of water storage locations in the bark. Water flows along water potential gradients and the depletion of a water storage location is always coupled with tissue shrinkage. Abbreviations: $\Delta\Psi_{XS}$ = water potential gradient between a lower tree section and the one illustrated; $\Delta\Psi_{AX}$ = water potential gradient between an upper tree section and the one illustrated; $\Delta\Psi_{XB}$ = water potential gradient between the bark (Ψ_B) and the wood (Ψ_X); and ΔR = stem radius fluctuation.

these slow-growing trees. It is therefore difficult, and in some cases impossible, to measure short-term growth rates with dendrometers.

Discussion

"Peristaltic" wave of storage depletion

In mature subalpine *P. abies* trees, internally stored water is successively depleted at ever-increasing distances from the crown periphery. This depletion of stored water, which is detected as a "peristaltic" wave of bark shrinkage along the stem and roots, can be plausibly modeled based on physical principles (Edwards et al. 1986, Tyree 1988). Zweifel (1999) simulated the fluctuations in stem radius of potted trees from the diurnal course of transpiration with such a model and we successfully applied a similar model to our mature trees. Transpiration draws water from the needles, which lowers the water potential within the foliage. The resulting water potential gradients serve as the accelerator for water movement within the tree, leading to depletion of water from internal storage locations in needles and bark (Hinckley et al. 1978). Water was more easily withdrawn from saturated internal water reserves close to the origin of water loss than from the soil, because of the force necessary to lift water from the soil to the crown and resistance in the flow path.

In Figure 5, the elastic water storage locations in the crown and bark are depicted as water-filled balloons along the flow path that shrink during periods of depletion and expand during periods of replenishment. Water in these storage locations is hydraulically connected to the water in the xylem and therefore contributes directly to transpiration during periods of depletion (Loustau et al. 1998). In *P. abies*, provided that the xylem water potential (Ψ_X) is higher than -2.3 ± 0.3 MPa, the volume change in storage tissues is proportional to the water exchange between bark and wood (Zweifel et al. 2000). The gradient between tracheids and each storage compartment ($\Delta\Psi_{XB}$) withdraws water from the bark. The gradient is composed of Ψ_X (next to the respective storage compartment), on the one hand, and the osmotic potential within the storage cells

and the mechanical expansion and contraction properties of the bark (Ψ_B), on the other hand. When Ψ_X decreases, the storage compartment shrinks and Ψ_B is lowered as the tissue contracts until Ψ_X and Ψ_B are in equilibrium ($\Delta\Psi_{XB} = 0$). Consequently, storage locations are fully replenished only when $\Delta\Psi_X$ reaches values close to zero or Ψ_B is additionally lowered by osmotically active substances. The amount of contraction of the bark tissue reflects the water potential status of the respective stem segment and provides a measure of tree water status (e.g., drought stress). Storage capacity, storage properties and flow resistance between bark and xylem together with the course of transpiration determine the diurnal dynamics of storage depletion and replenishment and the associated change in bark volume. Investigations on tomato plants have shown that not only bark and needles but also fruits can act as water storage locations. Ohta et al. (1997) measured the volume fluctuations of cherry tomatoes (*Lycopersicum* var. *cerasiforme* (Dunal)) and showed that, when the fruits shrink, the water they lose returns to the flow path of the plant and so contributes to transpiration. In this case, the analogy between a water storage location and an elastic water balloon is especially apt.

Response delay along the flow path

The delay in the onset of stem shrinkage in response to the onset of transpiration in the crown top cannot be characterized by a time constant per meter of flow path. This is because every tree section has its own dynamics and the response delay factor (rdf) also varies daily with changing environmental conditions (Figure 3). Variation in rdf can be explained through the functionality of internal water reserves. Three main factors are involved in the rdf of each tree section: flow resistances, storage capacities and transpiration. Flow resistances and storage capacities of bark and foliage within a tree section increase the

response delay, whereas transpiration of branches in lower tree sections reduces it.

Figure 6 shows the estimated values of the factors determining rdf in tree A for a partially sunny day. Bark storage capacity and rdf were calculated from measurements (Figure 3 and Tables 2 and 3), whereas flow resistance and crown storage capacity were estimated indirectly to fit these numbers to the measured rdf. Thus, transpiration of each crown section was assumed to be the difference between rdf and storage capacities + flow resistances. Flow resistances are reported to be highest near needles and in roots (Sellin 1993, Larcher 1995); however, this topic remains controversial. For example, Mencuccini and Grace (1996) reported that when values were integrated at the tree scale, most of the resistance was found in the stem, especially in large mature trees. In contrast, our measurements and model simulations indicated a higher flow resistance in branches and roots than in the stem.

Crown storage capacity was approximated from published biomass data for this tree species (Häsler et al. 1991, Herzog et al. 1998), assuming that crown storage capacity is proportional to needle biomass. Figure 6 shows that, in the upper tree sections, rdf (solid bar) could be much larger, because of the large water storage capacity of the crown, if there were no transpiration in the lower tree sections (horizontal arrows); i.e., transpiration considerably shortens the response delay. The higher the transpiration rate in the morning in the lower tree sections, the shorter the response delay. This is because transpiration depletes the water storage locations in the lower tree sections before the "peristaltic" wave, initiated at the treetop, reaches this part of the stem. The most extreme response delays were observed on mornings after rain or fog when internal water reserves were saturated. In these cases, the morning sun first dries up the superficially intercepted water in the upper crown, whereas the lower crown remains wet (Herzog et al. 1998). Under these conditions, transpiration occurred for a certain time only at the treetop and was not initiated in the lower parts, resulting in a distinctive "peristaltic" wave. If transpiration initially increased at the same time all over the tree, it is possible that stem shrinkage would occur first in the lower tree sections, especially if there was only a small storage capacity between the location of transpiration and the measurement point of the dendrometer on the stem. We conclude, therefore, that a short response delay between two tree sections does not unequivocally indicate that flow resistance is low or that the storage pools are small or empty. Instead, it could indicate that transpiration within the lower tree sections was initiated at the same time as at the treetop.

The situation in the roots differed from that in the above-ground biomass. Roots are connected in parallel, not in series, to the flow system and the water from roots flows together at the stem base. Roots do not transpire and, compared with the crown, they have only a small storage capacity because they lack needles. The large rdf in a small root in tree A (see Figure 6) must therefore have been caused primarily by a higher flow resistance in this root than in neighboring roots, assuming that root diameter mainly determines flow resistance. This assumption could explain why water flow and the measured contraction in radius along small roots exhibited such a large response delay compared with the response delay in the stem.

Storage depletion and replenishment

Depletion of stored water in the morning occurs in a regular succession along the stem, whereas replenishment of stored water in late afternoon exhibits no such regularity. In contrast to the expected replenishment of the bark beginning at the stem base and in the roots, the initial filling process was sometimes observed to occur first in the upper crown. Based on the functionality of our model, we postulate that refilling does not necessarily occur at the stem base first when the flow resistance between tree sections is high enough to confer some autonomy to every section. Thus, it is possible that transpiration in one (shaded) crown part has already ceased and replenishment in this tree section starts as a consequence of a reversed water potential gradient, whereas other tree parts still have high transpiration rates and remain in the storage-depleting status. It is also possible that products assimilated from photosynthesis are not evenly distributed within the phloem along the stem and that osmotic potential is increased more in certain stem sections than in other stem sections. The increase in osmotic potential in the bark lowers Ψ_B and could accelerate the initial rehydration process in the upper crown part. Notwithstanding these possible explanations, we cannot exclude the possibility that our observations of the onset of storage replenishment in different stem sections were an artifact, especially in those cases where the time delay was only few minutes. The smooth transition between depletion and replenishment (Figure 2) made it difficult to assign an exact time to the onset of replenishment.
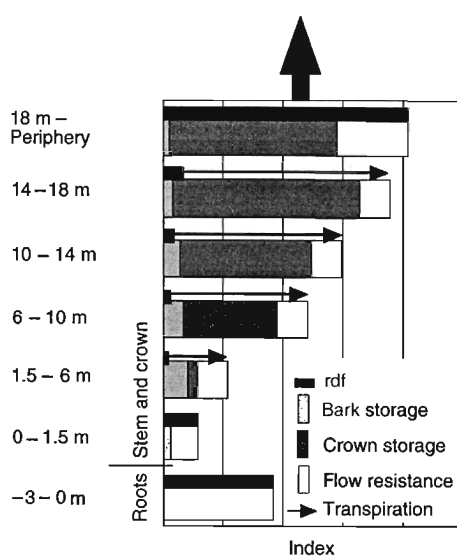

Figure 6. Comparison of the response delay factor (rdf) with the relative amounts of bark storage, crown storage and flow resistance in seven sections of tree A. The vertical arrow represents transpiration from the crown section between 18 m above ground and the crown periphery. The horizontal arrows indicate transpiration in the lower sections.

Quantification of storage locations

On a sunny day, water from the bark of our mature study trees contributed a maximum of 2 to 5 l to transpiration, depending on tree size (Table 3). This amount corresponds to about 5% of the transpiration of a mature *P. abies* over 1 day (Herzog et al. 1995, Wullschleger et al. 1998). This value is comparable with the 2–5% reported for young *P. abies* trees (Zweifel 1999) and the model calculations of 6–19% for *Thuja occidentalis* L. (Tyree 1988). Several studies have shown that the major part of internally stored water is withdrawn from the foliage (between 65 and 85%) and not from the bark (Edwards et al. 1986, Tyree 1988, Zweifel 1999). Consequently, the contribution of 5 l of water from the bark to transpiration can be supplemented by approximately 10 to 35 l of water withdrawn from the needles. The tenfold larger stem radius fluctuations in winter than in summer (Figure 4) are also a result of changing water contents in the bark. Freezing processes and their effects on stem radius fluctuations are discussed in detail in Zweifel and Häsler (2000).

Application of dendrometers

The ratio between the amount of water-induced stem radius change and growth-induced stem radius change also determines whether wood growth can be determined by measuring stem radius changes. In our study trees, water-induced changes in stem radius were up to twice as large as growth-induced changes in stem radius (Table 2). In spring, it is almost impossible to determine when wood growth starts in subalpine *P. abies* because of the simultaneous replenishment of water in the bark, which is severely dehydrated over winter (Zweifel and Häsler 2000).

However, because the diurnal course of stem radius change is a sensitive indicator of the sum of all the external and internal factors determining tree water relations, the dendrometer is a powerful instrument for investigating tree water relations. Although availability of soil water determines the upper limit of tree water potential, vapor pressure deficit of the air and radiation are the main driving forces of the diurnal course of transpiration and consequently of fluctuations in stem radius. These combined external factors influence internal water storage and, depending on the saturation status of each storage pool, different diurnal courses of stem radius change develop. Thus, individual reactions to external impacts determined by a single dendrometer applied to the stem might be useful for detecting stress in trees.

References

Boyce, R.L., A.J. Friedland, E.T. Webb and G.T. Herrick. 1991. Modeling the effect of winter climate on high elevation red spruce shoot water contents. For. Sci. 37:1567–1580.

Dobbs, R.C. and D.R.M. Scott. 1971. Distribution of diurnal fluctuations in stem circumference of Douglas-fir. Can. J. For. Res. 1: 80–83.

Edwards, W.R.N., P.G. Jarvis, J.J. Landsberg and H. Talbot. 1986. A dynamic model for studying flow of water in single trees. Tree Physiol. 1:309–324.

Forster, T., F.H. Schweingruber and B. Denneler. 2000. Increment puncher—a tool for extracting small cores of wood and bark from living tree. IAWA J. 21:169–180.

Früh, T. 1995. Entwicklung eines Simulationsmodells zur Untersuchung des Wasserflusses in der verzweigten Baumarchitektur. Selbstverlag des Forschungszentrums Waldökosysteme der Universität Göttingen, Göttingen, 192 p.

Gensler, W. and F. Diaz-Munoz. 1983. Stem diameter variations in cotton under field conditions. Crop Sci. 23:907–912.

Granier, A. 1985. Une nouvelle méthode pour la mesure du flux de sève brute dans le tronc des arbres. Ann. Sci. For. 42:193–200.

Gross, K. and W. Koch. 1991. Water relations of *Picea abies*. II. Determination of the apoplastic water content and other water relations parameter of needles by means of capillary microcryoscopy and pressure–volume analysis. Physiol. Plant. 83:296–303.

Häsler, R., C. Savi and K. Herzog. 1991. Photosynthese und stomatäre Leitfähigkeit unter dem Einfluss von Witterung und Luftschadstoffen. *In* Luftschadstoffe und Wald, Bd. 5, Ergebnisse aus dem Nationalen Forschungsprogramm 14. Ed. M. Stark. Verlag Fachvereine, Zürich, pp 143–168.

Herzog, K.M., R. Häsler and R. Thum. 1995. Diurnal changes in the radius of a subalpine Norway spruce stem: their relation to the sap flow and their use to estimate transpiration. Trees 10:94–101.

Herzog, K.M., R. Thum, G. Kronfuss, H.J. Heldstab and R. Häsler. 1998. Patterns and mechanisms of transpiration in a large subalpine Norway spruce (*Picea abies* (L.) Karst.). Ecol. Res. 13: 105–116.

Herzog, K.M., R. Thum, R. Zweifel and R. Häsler. 1997. Heat balance measurements: to quantify sap flow in thin stems only. Agric. For. Meteorol. 83:75–94.

Hinckley, T.M., J.P. Lassoie and S.W. Running. 1978. Temporal and spatial variations in the water status of forest trees. Society of American Foresters, Washington, DC, 74 p.

Irvine, J. and J. Grace. 1997. Continuous measurements of water tensions in the xylem of tree based on the elastic properties of wood. Planta 202:455–461.

Jarvis, P.G. 1975. Water transfer in plants. *In* Heat and Mass Transfer in the Environment of Vegetation. Eds. D.A. de Vries and N.H. van Alfen. Scripta Book Co., Washington, DC, pp 369–394.

Köstner, B., E.M. Falge, M. Alsheimer, R. Geyer and J.D. Tenhunen. 1998. Estimating tree canopy water use via xylem sap flow in an old Norway spruce forest and a comparison with simulation-based canopy transpiration estimates. Ann. Sci. For. 55:125–139.

Larcher, W. 1995. Physiological plant ecology. Springer-Verlag, Berlin, Heidelberg, New York, 506 p.

Loustau, D., J.C. Domec and A. Bosc. 1998. Interpreting the variations in xylem sap flux density within the trunk of maritime pine (*Pinus pinaster* Ait.): application of a model for calculating water flows at tree and stand levels. Ann. Sci. For. 55:29–46.

Mencuccini, M. and J. Grace. 1996. Developmental patterns of above-ground hydraulic conductance in a Scots pine (*Pinus sylvestris*) age sequence. Plant Cell Environ. 19:939–948.

Molz, F.J. and B. Klepper. 1973. On the mechanism of water-stress-induced stem deformation. Agron. J. 65:304–306.

Nakayama, F.S. and W.L. Ehrler. 1963. Beta ray gauging technique for measuring leaf water content changes and moisture status of plants. Plant Physiol. 38:95–98.

Ohta, K., T. Hosoki, K. Matsumoto, M. Ohya, N. Ito and K. Inaba. 1997. Relationships between fruit cracking and changes of fruit diameter associated with solute flow to fruit in cherry tomatoes. J. Jap. Soc. Hortic. Sci. 65:753–759.

Sellin, A. 1993. Resistance to water flow in xylem of *Picea abies* (L.) Karst. trees grown under contrasting light conditions. Trees 7: 220–226.

Siau, J.F. 1984. Transport processes in wood. Springer, Berlin, 142 p.

Tyree, M.T. 1988. A dynamic model for water flow in a single tree: evidence that models must account for hydraulic architecture. Tree Physiol. 4:195–217.

Williams, M., E.B. Rastetter, D.N. Fernandes et al. 1996. Modelling the soil–plant–atmosphere continuum in a *Quercus–Acer* stand at harvard forest: the regulation of stomatal conductance by light, nitrogen and soil/plant hydraulic properties. Plant Cell Environ. 19:911–927.

Wullschleger, S.D., F.C. Meinzer and R.A. Vertessy. 1998. A review of whole-plant water use studies in trees. Trees 18:499–512.

Zweifel, R. 1999. The rhythm of trees—water storage dynamics in subalpine Norway spruce. Diss. ETH Zürich No. 13391, 112 p.

Zweifel, R. and R. Häsler. 2000. Frost-induced reversible shrinkage of bark of mature, subalpine conifers. Agric. For. Meteorol. 102: 213–222.

Zweifel, R., H. Item and R. Häsler. 2000. Stem radius changes and their relation to stored water in stems of young Norway spruce trees. Trees 15:50–57.